PHYSICAL REVIEW B VOLUME 44, NUMBER 6 1 AUGUST 1991-II

Point-defect interactions when annealing diamonds implanted at low temperatures

Johan F. Prins
Schonland Research Center for Nuclear Sciences, University of the Witwatersrand, Johannesburg 2050, South Africa
(Received 18 October 1990; revised manuscript received 4 April 1991)

In this paper, the point-defect interactions which occur during annealing, when doping diamond by means of the cold-implantation–rapid-annealing technique [Phys. Rev. B **38**, 5576 (1988)], are modeled using reaction-rate theory. The equations predict that the magnitudes of the activation energies, controlling dopant–interstitial-vacancy combination and dopant-interstitial diffusion, relative to the same energies applicable to the self-interstitials, determine the end result which will be obtained for a chosen implantation-annealing sequence. It is also possible to explain why an increase in the annealing temperature can lead to a decrease in dopant activation, as had been observed experimentally (and reported elsewhere) for boron. Reasonable values for the self-interstitial activation energies are found when applying this model to previously published results.

I. INTRODUCTION

Doping of diamond by means of ion implantation has been attempted since the early 1960s. One aspect which complicated the interpretation of results has been the thermodynamic metastability of this material. It is now clear that some of the earlier claims to success, which even led to a patent application,[1] can be ascribed to radiation damage. The vacancies are known to be optically active in diamond[2] and are believed to act as donors which can compensate acceptor centers.[3,4] Above room temperature self-interstitials can diffuse during ion implantation.[5,6] When they diffuse out of the layer, being implanted, an excess of vacancies is left behind, which lowers the material density and thus promotes the formation of more complex defect structures or even graphitization during subsequent annealing. From this realization a doping procedure was developed which entailed cooling of the diamond substrate to a low temperature (typically liquid nitrogen) to inhibit interstitial diffusion, followed by annealing at a suitable high temperature to induce interstitial-vacancy annihilation.[7,8]

During the annealing stage, dopant atoms, which combine with vacancies, become activated (provided that they are substitutional dopants) and self-interstitials recombining with vacancies diminish the radiation damage. Obviously, some of the self-interstitials can still diffuse from the ion-damaged layer to leave vacancies behind. It was found that the residual radiation damage, after annealing, form deep-lying donor centers at ≈ 4 eV below the conduction band.[7] From a statistical analysis of the electrical conduction of boron-doped layers, which were heavily compensated by these deep-lying donor centers, it was found that the donors have extremely large degeneracy weighting factors which depend on the annealing cycle employed.[9] To explain this phenomenon it was tentatively proposed that the donors result from the agglomeration of vacancies to form "vacancy crystallites," which effectively maintain the electronic characteristics of the single vacancy in a narrow energy-band structure. For the latter reason these donors were termed "vacloids" in order to distinguish them from the standard concept attributed to vacancy clustering in other materials.

Initially, a simple, intuitive model was derived to describe the above-mentioned cold-implantation–rapid-annealing (CIRA) process and applied to doping when using boron ions.[7] It was assumed that each interstitial (self-interstitials as well as the implanted boron atoms) has a certain probability P during annealing to encounter and combine with a vacancy before it can diffuse out of the implanted layer. From previous experience[6] the assumption was made that this probability is proportional to the atomic vacancy density C_v and the width of the ion-implantation-damaged layer ω, such that it may be written as

$$P = \beta\omega C_v = \frac{\beta n_v}{N} , \tag{1}$$

where n_v is the number of vacancies per cm^2, N the atomic density per cm^3 of atoms in a perfect diamond crystal, and β a proportionality constant which increases with temperature for self-interstitials.[10] Obviously, β should depend on the type of interstitial involved. Because carbon and boron are next to each other in the periodic table, it was assumed that β would roughly be the same for both types of atoms.[7,9] Inherent in this approach is the further assumption that the self-interstitials and boron interstitials are distributed in the same manner among the vacancies. This is not true when implanting only boron at a single energy. The situation can be amended by either coimplanting carbon ions, to create the damaged structure into which the boron is then implanted, or by implanting boron at a series of different energies to force overlapping distributions over a wider width ω.

Recent experiments, employing different initial annealing temperatures on identically implanted diamonds, showed clearly that the carbon and boron interstitials do not behave in a similar fashion, even though coimplanta-

 ©1991 The American Physical Society

tions were used to ensure similar spatial distributions.[11] Although self-interstitial–vacancy recombination improved with increasing annealing temperature, boron-interstitial–vacancy combination became worse. In terms of the simple probability function used in Eq. (1), this would indicate that, in contrast to carbon interstitials, β decreases with increasing temperature for boron. The increase in β for the carbon-interstitial–vacancy combination indicates that an activation energy must be operative for this process. Similarly, an activation energy would be expected for the boron-interstitial–vacancy combination reaction. It is, of course, possible that the reaction rates, at a chosen temperature, could favor one process above the other if their "chemical" reaction constants, which depend, *inter alia,* on the activation energies, differ. Clearly, a more fundamental description of the point-defect interactions, which are operative during annealing, is needed.

In this paper a theoretical model for the point-defect interactions is derived from reaction-rate equations and applied to some of the experimental results which have been observed when doping diamond layers by means of the CIRA method. From this, a deeper insight into the role of the different activation energies can be gained, and this, in turn, should assist in developing better annealing cycles in the future.

II. THEORETICAL MODEL

A. Rate equations

Implantation is carried out at a low enough temperature to "freeze" in the intrinsic and implanted point defects,[7] thus preventing them from diffusing. In this process, n_{v0} vacancies, n_{i0} carbon interstitials, and n_{d0} dopant atoms are introduced per cm^2 into the ion-implanted layer of width ω. Because of the large number of self-interstitials created in the collision cascade of a single ion,

$$n_{d0} \ll n_{i0} \approx n_{v0} . \tag{2}$$

After implantation, the diamond is rapidly heated to a suitable annealing temperature, at which the point defects may diffuse and combine. Self-interstitials, combining with vacancies, reduce the radiation damage, and dopant interstitials, doing the same, become activated. At time t there will be n_v vacancies, n_i self-interstitials, and n_d dopant interstitials per cm^2 in the implanted layer of width ω. The rate R_c at which recombination occurs will be assumed to be proportional to the density of each reactant to the first order and may thus be written for the self-interstitial–vacancy reaction as

$$R_c = \frac{\kappa n_v n_i}{\omega^2} , \tag{3}$$

where κ is the rate constant which is assumed to follow an Arhenius relationship with an activation energy E_C, such that

$$\kappa = \kappa_0 \exp\left[-\frac{E_C}{kT}\right] . \tag{4}$$

As usual, k is Boltzmann's constant and T the absolute temperature.

However, at the same time, some of the self-interstitials also diffuse out of the damaged layer at a rate R_e. It seems reasonable to assume that this factor should be proportional to the density of the self-interstitials and inversely proportional to the width ω. Accordingly,

$$R_e = \frac{\varphi n_i}{\omega^2} , \tag{5}$$

where φ is a proportionality constant which will increase with temperature. From diffusion theory the average time needed for a diffusing entity to move through a distance ω follows as ω^2/D, where D is the diffusion coefficient. φ should thus be proportional to D and should increase with temperature subject to the same activation energy E_D; which leads to the relationship

$$\varphi = \varphi_0 \exp\left[-\frac{E_D}{kT}\right] . \tag{6}$$

The rate at which the self-interstitials decrease during the anneal is thus given by the sum of R_c and R_e, leading to the equation

$$\frac{dn_i}{dt} = -n_i \left[\frac{\kappa n_v + \varphi}{\omega^2}\right] . \tag{7}$$

The corresponding equation for n_d is

$$\frac{dn_d}{dt} = -n_d \left[\frac{\kappa_d n_v + \varphi_d}{\omega^2}\right] , \tag{8}$$

where the subscripted d parameters are defined similarly to the corresponding unsubscripted parameters with temperature dependences characterized by activation energies E_{Cd} and E_{Dd} as in Eqs. (4) and (6).

If the temperature is high enough, the vacancies can also diffuse. Of the vacancies which did not combine with interstitials, some may also escape from the ion-damaged width ω, while others may interact to form the deep-lying donor centers which had been deduced from experiment.[7,10] If one assumes an instantaneous heating to a temperature at which all the point defects can diffuse and interact, corresponding equations for the vacancies need to be considered. However, taking the present rapid-annealing technology into account, the rate of heating probably ensures that the interstitials (or at least the self-interstitials) will have diffused, recombined, and escaped long before significant vacancy diffusion has occurred. Although the possibility exists that, for certain dopants, diffusion of the dopant interstitials may only become significant at the same, or even higher, temperatures than vacancy diffusion, the assumption, in this analysis, will be made that the self-interstitial and dopant diffusion-combination reactions effectively exhausted themselves before significant vacancy diffusion and agglomeration can occur. Accordingly, the decrease in vacancies, caused by combining with the interstitials, follows from Eq. (3) and the equivalent expression for the

dopant atoms as

$$-\frac{dn_v}{dt}=\frac{\kappa n_v n_i}{\omega^2}+\frac{\kappa_d n_v n_d}{\omega^2} . \tag{9}$$

B. Interstitial-vacancy equation

With the assumptions made above, the interstitial-vacancy interactions will dominate the annealing process up to the point where the residual vacancy-vacancy interactions remain. To determine the number of residual vacancies, which did not combine with interstitials, Eq. (9) has to be solved. If one assumes that $n_d \ll n_i$ [see Eq. (2)], during the largest part of the annealing cycle, the second term in Eq. (9) may be neglected and the main governing equation derived by eliminating n_i, with the aid of Eq. (7), which then renders

$$\left[1+\frac{\varphi}{\kappa n_v}\right] dn_v = dn_i . \tag{10}$$

Integration leads to the change of n_{v0} to n_v for the corresponding change of n_{i0} ($\approx n_{v0}$) to n_i and gives the relationship

$$n_i = n_v - \frac{\varphi}{\kappa}\left[\frac{n_{v0}}{n_v}\right] . \tag{11}$$

At the end of the annealing phase, $n_i \approx 0$, which leads to the number of residual vacancies n_{vf} as

$$\frac{n_{vf}}{n_{v0}} = \exp\left[-\left[\frac{\kappa n_{v0}}{\varphi}\right]\left[\frac{n_{vf}}{n_{v0}}\right]\right] . \tag{12}$$

Obviously, when n_{vf} becomes very small, the effect of n_d may become non-negligible, especially if n_{vf}, as determined by Eq. (12), becomes comparable to, or smaller than, the number of dopants activated. However, in the doping experiments done to date, using boron, the indications strongly suggest that n_{vf} is large enough to validate the use of Eq. (12).[7–9,11,12]

For given values of κ, φ, and n_{v0}, Eq. (12) can be solved by iteration. The following substitutions are made to follow the relevant behavior of this equation and to facilitate later discussion:

$$Y = \frac{n_{vf}}{n_{v0}} \tag{13}$$

and

$$X = \frac{\kappa n_{v0}}{\varphi} , \tag{14}$$

which give

$$X = -\frac{\ln Y}{Y} , \tag{15}$$

for Eq. (12). Obviously, $0 < Y < 1$ because $n_{vf} < n_{v0}$. In Fig. 1 it can be seen that Y decreases with increasing X, i.e., with increasing κ/φ or n_{v0}. Experimental results[11] indicate that n_{vf} decreases with increasing annealing temperature for the same n_{v0}, which can only mean that κ/φ increases with temperature or, according to Eqs. (4) and (6), that $E_C > E_D$.

C. Interstitial decay times

It is an interesting and useful exercise to assume that the decay of the self-interstitials n_i may be described in terms of an average lifetime τ_i, allowing one to write

$$n_i = n_{v0}\exp\left[-\frac{t}{\tau_i}\right] . \tag{16}$$

Substituting this expression into Eq. (9) and integrating gives a time-dependent expression for n_v, i.e.,

$$n_v = n_{v0}\exp\left\{\frac{\kappa n_{v0}\tau_i}{\omega^2}\left[\exp\left[-\frac{t}{\tau_i}\right]-1\right]\right\} , \tag{17}$$

which for $t \gg \tau_i$ becomes

$$n_{vf} = n_{v0}\exp\left[-\frac{\kappa n_{v0}\tau_i}{\omega^2}\right] . \tag{18}$$

Comparing the latter equation with the equivalent Eq. (12) leads to an expression for τ_i:

$$\tau_i = \left[\frac{\omega^2}{\varphi}\right]\left[\frac{n_{vf}}{n_{v0}}\right] . \tag{19}$$

In other words, the time constant ω^2/φ, which may be considered as the average time it will take an interstitial

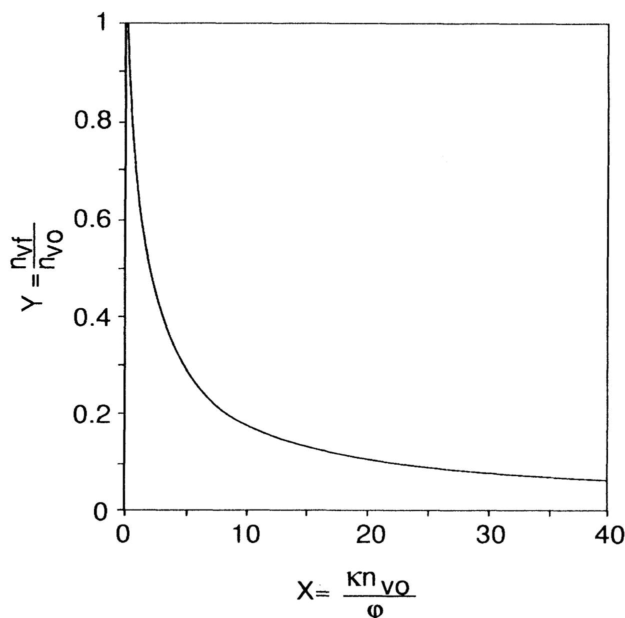

FIG. 1. Fraction Y of residual, uncombined vacancies n_{vf} to the original density n_{v0}, as a function of $X = \kappa n_{v0}/\varphi$, where κ is the reaction-rate parameter for interstitial-vacancy recombination and φ the diffusion constant for self-interstitial diffusion.

to diffuse out of the layer when no vacancies are present, becomes contracted to τ_i. It is not surprising that the presence of the vacancies should shorten the average lifetime, and Eq. (19) thus seems a reasonable result.

The relationship between n_i and n_d at time t may be found by combining Eqs. (7) and (8) through the elimination of n_v. This leads to the differential equation

$$\frac{dn_i}{\kappa n_i}-\frac{dn_d}{\kappa_d n_d}=\omega^{-2}\left[\frac{\varphi_d}{\kappa_d}-\frac{\varphi}{\kappa}\right]dt\ . \tag{20}$$

Integration and substitution for n_i from Eq. (16) give

$$n_d=n_{d0}\exp\left\{-\left[\omega^{-2}\left[\varphi_d-\frac{\kappa_d\varphi}{\kappa}\right]+\frac{\kappa_d}{\kappa\tau_i}\right]t\right\}\ . \tag{21}$$

Thus, at a single temperature, the dopant interstitials may also be considered to decay with a simple time constant τ_d, where

$$\tau_d=\left[\frac{\omega^2}{\varphi_d}\right]\left[1+\frac{\phi}{\Gamma}\right]^{-1}\ . \tag{22}$$

The functions Γ and ϕ follow as

$$\Gamma=\left[\frac{\kappa\varphi_d}{\kappa_d\varphi}\right] \tag{23}$$

and

$$\phi=\left[\frac{n_{v0}}{n_{vf}}-1\right]\ . \tag{24}$$

In the derivation of these equations, the parameter τ_i in Eq. (21) was replaced with the expression in Eq. (19). As one would expect, the lifetime of the dopant interstitials is also shortened by the presence of the vacancies.

D. Activation ratio

Each dopant interstitial which combines with a vacancy becomes activated. If at time t, n_{da} dopants have been activated, the second term in Eq. (9) may be written as dn_{da}/dt. Combining this fact with Eq. (8) renders

$$dn_{da}=-dn_d-[\varphi_d\omega^{-2}n_d\,dt]\ . \tag{25}$$

Substituting for n_d and dn_d, with the aid of Eqs. (21) and (22), and integrating over a time $t\gg\tau_d$ lead to the simple result that

$$n_{da}=n_{d0}\left[1-\frac{\tau_d\varphi_d}{\omega^2}\right]\ . \tag{26}$$

The smaller the decay time τ_d becomes relative to the vacancy-free escape time ω^2/φ_d, the more dopants will be activated. By replacing τ_d in Eq. (26) with the expression in Eq. (22), the dopant activation ratio becomes

$$R_A=\frac{n_{da}}{n_{d0}}=\left[1+\frac{\Gamma}{\phi}\right]^{-1}\ . \tag{27}$$

In order to improve the activation ratio R_A, Γ/ϕ has to be made as small as possible. As already mentioned above, $Y=n_{vf}/n_{v0}$ decreases with increasing temperature. Accordingly, the factor ϕ in Eq. (24) will increase. If, as for boron dopants, R_A decreases with increasing temperature,[11] it would mean that the factor Γ in Eq. (23) increases faster with temperature than ϕ. From Eqs. (4), (6), and the equivalent expressions for the dopant atoms, Γ may be written as

$$\Gamma=\left[\frac{\kappa_0\varphi_{d0}}{\varphi_0\kappa_{d0}}\right]\exp\left[\frac{(E_C-E_D)-(E_{Cd}-E_{Dd})}{kT}\right]\ . \tag{28}$$

Clearly, this parameter can only increase with temperature if

$$E_\Gamma=(E_C-E_D)-(E_{Cd}-E_{Dd})>0\ , \tag{29a}$$

i.e.,

$$\Delta E=E_C-E_D>\Delta E_d=E_{Cd}-E_{Dd}\ , \tag{29b}$$

where it is known that $\Delta E\geq 0$ (see Sec. II A).

III. APPLICATION TO EXPERIMENTAL RESULTS

The model, derived above, emanated from the desire to explain why the behavior of boron interstitials differs from that of self-interstitials when annealing ion-implanted diamond layers.[11] A summarized, pictorial representation of this difference is shown in Fig. 2.[11,12] Two curves, each for equivalently ion-damaged diamonds, show the change in resistance (measured at a single temperature) as a function of the first temperature to which the diamonds were rapidly heated after ion implantation at −196 °C. One set of data is for diamonds implanted with only carbon ions, while the other is for coimplanted carbon and boron ions. During the first part of the annealing cycle, each diamond was held at its preselected temperature for 1 h. This was followed by a further anneal at 1170 °C for another hour. Rapid heating was effected by sliding the diamonds down an inclined chute into a preheated graphite crucible.[11]

The energies and doses employed for the diamonds, which were identically coimplanted with carbon and boron ions (lower curve in Fig. 2), are shown in Table I. Added to this table are the expected average number of vacancies per ion, for each ion and energy, as generated by the computer program TRIM89.[13] The displacement energy was assumed to be 55 eV[6] for the carbon atoms in the diamond lattice. According to this calculation, $n_{v0}\approx 7.3\times 10^{17}$ cm^{-2}. For the second curve (Fig. 2), the carbon-ion doses were spread over the same energies shown in Table I, but were slightly increased to keep n_{v0} the same as for the coimplanted specimens.

The conduction, measured for the carbon-only implanted layers in Fig. 2, must be caused by the residual radiation damage after annealing, and this is clearly decreasing with increasing annealing temperature, commensurate with better self-interstitial-vacancy recombination. Less vacancies are available to form deep-lying donor centers. In contrast, the boron-doped layers show a minimum in the resultant electrical resistances. A parabola was fitted to the four lowest-temperature points,

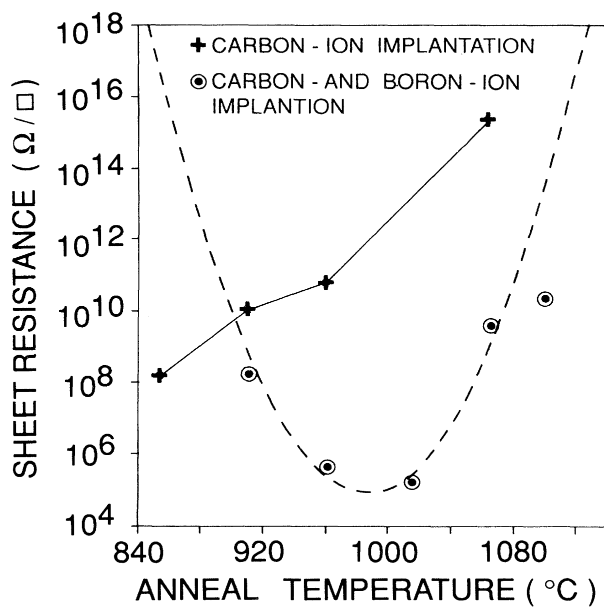

FIG. 2. Comparison of the change in sheet resistance with the first annealing temperature, when using a two-stage annealing cycle, after cold-target implantation. The doses used for the coimplanted B^+ and C^+ layers are shown in Table I. For the carbon-only implanted layers, the carbon-ion doses in Table I were slightly increased to generate the same initial density of vacancies. Whereas the carbon-only implanted layers gave an increasing sheet resistance with annealing temperature, the boron-coimplanted layers show a minimum resistance at about 1000 °C. A parabola was fitted to the four points measured for the layers (annealed at the lowest temperatures), which all showed variable-range-hopping conduction (see also Fig. 8). The sheet resistances displayed for the carbon-only layers were measured at 150 °C and for the coimplanted layers at 40 °C (from Refs. 11 and 12).

which indicated that the minimum occurred at ≈986 °C. (The reason why the fifth point was ignored is discussed later in the text.) As the compensating donors are decreasing with increasing annealing temperature, the minimum can only be caused by a concomitant decrease

TABLE I. Ion energies and doses which were used to create an intermixed distribution of radiation damage and boron atoms over the whole width of the implanted layer.

Ion	Energy (keV)	Dose (cm^{-2})	Vacancies (cm^{-2})
Carbon	150	2.06×10^{15}	3.19×10^{17}
	120	1.34×10^{15}	1.94×10^{17}
	80	1.13×10^{15}	1.36×10^{17}
	50	6.20×10^{14}	6.10×10^{16}
Total carbon-ion dose		5.15×10^{15}	
Boron	120	7.64×10^{13}	1.01×10^{16}
	75	5.68×10^{13}	6.34×10^{15}
	44	4.18×10^{13}	3.56×10^{15}
Total boron-ion dose		1.75×10^{14}	
Total vacancies n_{v0}			7.3×10^{17}

in the density of activated boron acceptors.[11,12]

When representing the change of sheet resistance R_s, for these implantation-annealed diamonds, as a function of absolute temperature T, it was found that large sections did not give linear relationships for $\ln(R_s)$ versus T^{-1}. The curves, for the carbon-only implantations, are shown in Fig. 3.[11] At high temperatures the two layers, annealed at 960 and 1065 °C, did, in contrast, show linear regions corresponding to an activation energy ≈4 eV. This is the energy expected when electrons are activated from vacloids to the conduction band. Furthermore, if one ignores the noise above 10^{14} Ω/□ for curve D (annealed at 1065 °C), the lower-temperature branch also appears linear with an activation energy of ≈1.1 eV. All the other curve sections and curves gradually increased their slopes toward smaller inverse temperatures, typically, as expected for variable-range-hopping conduction.[14,15] For this electrical conduction mechanism, the sheet resistance R_s follows Mott's law with temperature T; i.e.,

$$\ln(R_s)=\ln(R_{0s})+ST^{-1/n}, \tag{30}$$

where

$$S^n \propto \alpha^{n-1}/kN(E_F). \tag{31}$$

Here α^{-1} is a length approximating the extension of the

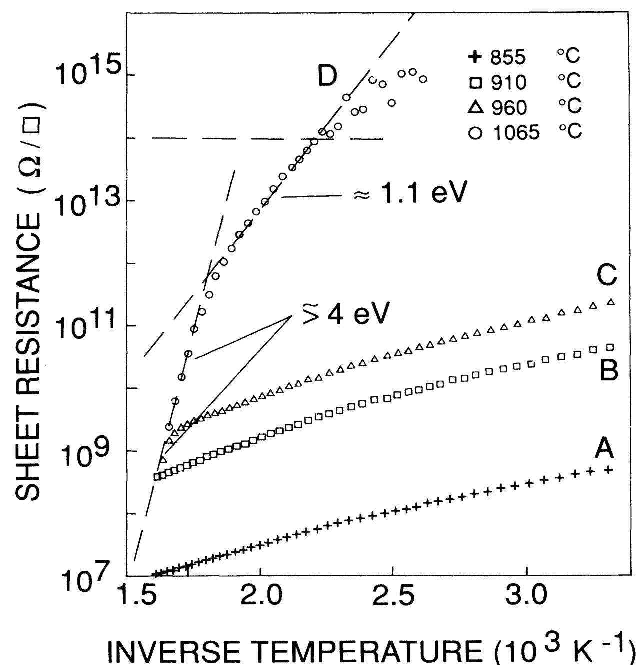

FIG. 3. Sheet resistance as a function of inverse temperature for the carbon-ion implanted diamond layers annealed at different initial temperatures. Curves A, B, and C indicate hopping conduction over the whole temperature range, except at high temperatures where, for C, an activation energy of ≈4 eV becomes prevalent. In contrast, curve D shows, essentially, two regions with activation energies of ≈4 and 1.1 eV (from Ref. 11).

localized wave function of a hopping center, k is Boltzmann's constant, and $N(E_F)$ is the density of hopping states near the Fermi level. For three-dimensional hopping, $n=4$. However, in a very thin layer, where the thickness becomes comparable with the hopping distance, two-dimensional hopping may occur, and then $n=3$.[15]

For the very high resistances shown in Fig. 3, the possibility of two-dimensional hopping should not be excluded. When plotting $\ln(R_s)$ against $T^{-1/4}$ as well as $T^{-1/3}$, both representations seem to give, within experimental error, linear relationships for the hopping parts of the data. Accordingly, it was decided to choose between the two possibilities by fitting Eq. (30) to the data, for both $n=4$ and 3, using the method of least squares. More data points were measured than the ones shown in Fig. 3, and all the data, recorded at every 2 °C interval, were used to calculate the best linear curves. Although curve D seems linear at lower temperatures, as discussed above, it was decided to calculate similar fits for its low-temperature branch. Only the data collected between $1000/T=2.0$ and 2.2 were used for this purpose. Similarly, owing to its linear behavior at high temperatures, only the data above $1000/T=1.8$ were used for the 960 °C curve (curve C). The results are summarized in Table II. The average least-squares deviation per data point, Σ_{av}, is also shown for each curve fitted. Except for the D curve, Σ_{av} was less for $n=4$, in each case, thus favoring three-dimensional hopping conduction. Accordingly, the data were interpreted for $n=4$, where the hopping-center density $N(E_F)$ can be taken as proportional to S^{-4} [see Eq. (30) and Table II].

For the data of curve D, as a function of T^{-1}, Σ_{av} decreased even further to 1.65×10^{-4}, giving a semiconducting activation energy of 1.07 eV. This value is near the energy of ≈ 1.23 eV found for charged vacloids above the valence band[9] and may thus be caused by the excitation of electrons from the latter band to such centers. In a case such as the present one, where donors overcompensate acceptor levels, the Fermi level should lie near the donor level, thus causing hole conduction with an activation energy of this approximate magnitude. Accordingly, it was decided not to try to fit any part of curve D to the hopping equation.

When, only, implanting carbon ions, the net result after annealing should be mainly (or, at least, according to the theory developed above, only) vacloids, which formed out of some of the residual number of uncombined vacancies n_{vf}. It is thus tempting to identify each hopping center, for the curves shown in Fig. 3, with a vacloid. However, the large degeneracy weighting factor[9] of these entities may amplify the number of hopping options. Furthermore, a study of the onset of hopping conduction in diamonds, implanted with carbon ions at a target temperature of 240 °C, which allowed interstitial diffusion during the process, indicated a correlation with the number of excess vacancies which remained after some interstitial outdiffusion.[5] Initially, the assumption will be made, albeit cautiously, that the number of hopping centers for the implanted layers of Fig. 3 (after the carbon-ion implantation and annealing) is directly proportional to the residual, uncombined vacancies n_{vf}. Obviously, it is more than likely that some of these vacancies diffused out of the layer and that the amount that escaped may also have been altered by the subsequent annealing step. It seems logical to expect that more vacancies will be able to escape, during both the annealing stages employed, for a smaller value of the uncombined density n_{vf}. Owing to the fact that v_{vf} decreases with increasing annealing temperature, more of these uncombined residuals should escape the higher the initial annealing temperature becomes. Thus, by assuming, as is done for this analysis, that the number of experimentally determined hopping centers correlates directly with the calculated amount of uncombined vacancies n_{vf}, the true number of uncombined vacancies may be progressively underestimated with increasing annealing temperature.

To determine whether the theoretical model, derived above, approaches a reasonable description of the experimental data, a correlation between the calculated values for n_{vf} and S^{-4} may be attempted. However, to do this the dependence of κ/φ, on the absolute temperature needs to be known [see Eq. (12) and Fig. 1]. In other words, the parameters κ_0, φ_0, and $\Delta E=E_C-E_D$ are needed according to Eqs. (4) and (6). At present, these parameters are unknown. In fact, their determination

TABLE II. Slopes S and the appropriate ratios which are proportional to the hopping-center density $N(E_F)$, when representing the sheet resistance data in Fig. 3 as a function of $T^{-1/n}$, for $n=3$ and 4. Σ_{av} is the average least-squares deviation obtained in each case.

	Curves in Fig. 3	A	B	C	D
n	Anneal temp. (°C)	855	910	960	1065
	Slope S	54.4	68.1	70.9	262.0
3	$S^{-3}\propto N(E_F)$	6.21×10^{-6}	3.17×10^{-6}	2.81×10^{-6}	5.56×10^{-8}
	S^{-3} ratios	1	0.51	0.45	0.0085
	Σ_{av}	1.82×10^{-4}	7.71×10^{-4}	4.30×10^{-4}	1.90×10^{-4}
	Slope S	43.7	54.8	57.1	202.0
4	$S^{-4}\propto N(E_F)$	2.74×10^{-7}	1.11×10^{-7}	9.41×10^{-8}	6.01×10^{-10}
	S^{-4} ratios	1	0.41	0.34	0.0022
	Σ_{av}	1.04×10^{-4}	5.37×10^{-4}	2.46×10^{-4}	1.93×10^{-4}

from the existing experimental data, in itself, will lend credence to the model if reasonable values are to be found. Accordingly, it was decided to develop a plausible correspondence between the theory and the data in Table II (for $n=4$) and then to judge whether the values for ΔE and the other constants are acceptable.

In order to work within an inverse temperature scale, Eq. (14) can be combined with Eqs. (4) and (6) to obtain the relationship

$$-\ln(X)=\frac{\Delta E}{kT}-\ln\left[\frac{\kappa_0 n_{v0}}{\varphi_0}\right]. \quad (32)$$

$Y=n_{vf}/n_{v0}$ is a function of X [see Eq. (15)] and thus also of $-\ln(X)$. The relationship between these two parameters can be seen in Fig. 4. If the theory is correct, all the possible values of n_{vf}, for a chosen n_{v0}, must fall on this curve. In terms of the crude assumptions, made above, S^{-4} is assumed to be proportional to n_{vf}. Accordingly, the data in Table II should also correlate with the curve in Fig. 4.

To place the data points on the latter curve, the position of at least one point is needed. By choosing a value $Y=Y_A$ for curve A between unity and zero, the corresponding Y values for the curves B and C could be calculated using the ratios of S^{-4} in Table II. From these numbers the values for $-\ln(X)$ could, in turn, be derived from Eq. (15). The linear expression [Eq. (32)] was then fitted to the latter data by using the least-squares deviation method. Y_A was systematically varied and the corresponding values for ΔE and $b=\ln(\kappa_0 n_{v0}/\varphi_0)$ determined in each case. At first, it was hoped that the average least-squares deviation Σ_{av} will change as a function of Y_A and reach a minimum, from which the most probable values for ΔE and b could be deduced. However, although a rapid decrease in Σ_{av} was found at high values for Y_A, the decrease flattened out at low values without ever reaching a minimum value. This behavior can be caused by the S shape of the curve in Fig. 4 if all the data points lie near to, or on, its lower leg.

Another method had to be found in order to select values for ΔE and b, which may be considered as reasonable. In Fig. 5, ΔE, b, Σ_{av}, and the slope of Σ_{av} are all shown as functions of Y_A on a logarithmic scale. The initial, rapid decrease in ΔE and b corresponds to the decrease in Σ_{av} and may be considered as an indication that these values for Y_A are too high. For small values of Y_A, the slope of Σ_{av} changes very little, showing a fairly sudden increase for values of $Y_A > 10^{-1.72}$. The slope increases then nearly linearly up to $Y_A \approx 10^{-1}$, from where it rapidly goes to very high values. From this behavior it seems that Σ_{av} approaches $Y_A \approx 10^{-1.72}$ parabolically when decreasing, indicating that the minimum point should have been at the latter position. Using this value, the corresponding values for ΔE and b are 1.52 eV and 21.10, respectively. However, to play safe, the slopes at high and low values of Y_A were extrapolated and their intersection at $Y_A \approx 10^{-0.56}=0.275$, used as another possibility. In this case the values for ΔE and b came to 1.95 eV and 21.73, respectively. The latter value for Y_A is probably a gross overestimation. In a previous assessment for a nearly similar implanted layer, annealed at a slower rate to 1200 °C, the self-interstitial activation ratio was estimated to be ≈ 0.96; i.e., $Y=n_{vf}/n_{v0}\approx 0.04$.[9] Accordingly, the appropriate value for Y_A will probably be

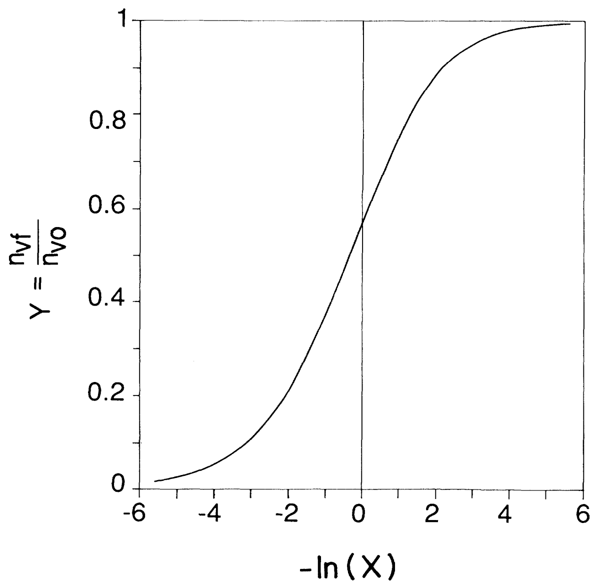

FIG. 4. Fraction Y of the uncombined vacancies n_{vf} to initial vacancies n_{v0}, as a function of $-\ln(X)$, where $X=\kappa n_{v0}/\varphi$. $-\ln(X)$ is linearly related to T^{-1}.

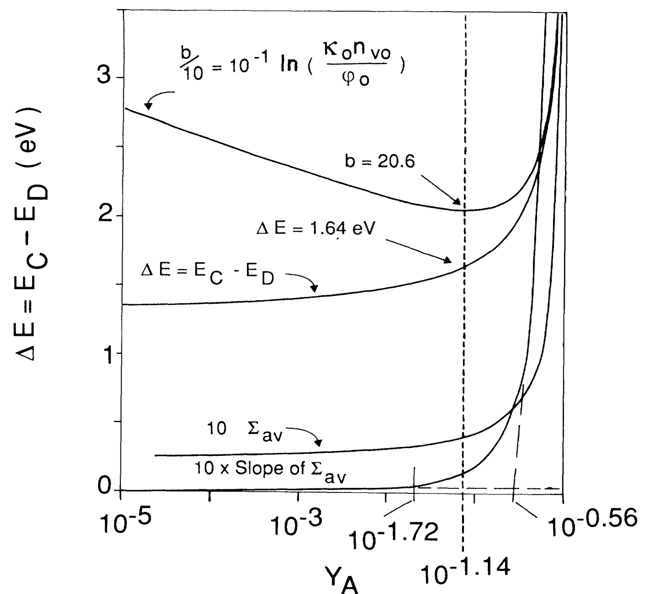

FIG. 5. Difference in interstitial-vacancy recombination energy E_C, and the self-interstitial diffusion energy E_D, as a function of the possible annealed vacancy fraction Y_A, for curve A in Fig. 2. On the same graph the average least-squares deviation Σ_{av} found for each value of Y_A is also shown, as well as the slope of the latter curve. The corresponding values for b [see Eq. (32)] can also be seen.

less than 0.1. Fortunately, the value of ΔE changes slowly for $Y_A < 0.1$, to flatten out at ≈ 1.3 eV for very small Y_A. One may thus safely assume that the analysis used places ΔE somewhere between 2 and 1.3 eV. It was decided to choose $Y_A = 10^{-1.14}$, which lies halfway between the two previous values and has the aesthetic appeal that the minimum value for b is selected (see Fig. 5). From this choice the corresponding values for ΔE and b follow as 1.64 eV and 20.60, respectively. Substituting these numbers into Eq. (32) and using Eq. (14) lead to

$$\frac{\kappa n_{v0}}{\varphi} = 8.84 \times 10^8 \exp\left[-\frac{1.64 \text{ eV}}{kT}\right] . \quad (33)$$

For $n_{v0} = 7.3 \times 10^{17}$ cm^{-2} (see Table I),

$$\frac{\kappa_0}{\varphi_0} = 1.21 \times 10^{-9} \text{ cm}^2 . \quad (34)$$

No experimental data exist which may be used to ascertain whether this value for κ_0/φ_0 is acceptable. However, it is pleasing that reasonable-looking values for ΔE could be found. From theoretical calculations the energy needed to create a vacancy in the diamond lattice is ≈ 7 eV.[16] One would expect E_C to be of the same order of magnitude but smaller. According to Clark and Palmer,[17] $E_D \approx 1.3$ eV, which renders a reasonably acceptable value for E_C of approximately 2.9 eV.

It is now possible to use Eq. (33) in conjunction with Eq. (12) to calculate the change in $Y = n_{vf}/n_{v0}$ as a function of annealing temperature. The behavior is shown in Fig. 6, which also shows the corresponding experimental points which were used to derive the curve. As expected, the relationship is not linear, but the deviation from linearity is gradual. Within a limited temperature range it is possible to extract an average "activation" energy. For example, the tangent (dotted line) at 900 °C has a slope of 1.31 eV.

As already mentioned, the function Γ [Eq. (28)] should change faster than ϕ [Eq. (34)] if the dopant activation ratio R_A decreases with increasing temperature. From the previous data, the behavior of ϕ with temperature can be determined, and the result, over a wide temperature range, is shown in Fig. 7. The slope of $\ln(\phi)$ versus inverse temperature is highest (≈ 1.62 eV) and fairly constant at lower temperatures. Γ can only increase faster if its slope is higher. Accordingly, $E_\Gamma > 1.62$ eV, which, from Eq. (29) and $\Delta E = 1.64$, gives $\Delta E_d < 0.02$ eV. It is thus possible that ΔE_d may even be negative, in which case $E_{Dd} > E_{Cd}$.

The ultimate next step would be to determine the corresponding values ΔE_d and κ_{0d}/φ_{0d} for the boron-implanted interstitials. For the boron-doped layers, implanted to the doses shown in Table I and annealed to different temperatures, the change is resistance as a function of inverse temperature is shown in Fig. 8.[11] Except for the layer annealed at 1100 °C, which shows a linear portion with an activation energy of ≈ 0.37 eV, as expected for hole conduction in the valence band, all the other layers have changing slopes indicative of variable-range-hopping conduction. In the latter cases, one may make the reasonable assumption that the density of hopping centers is proportional to the density of uncompensated boron acceptors. In each case the number of boron acceptors n_A per cm^2 follows as

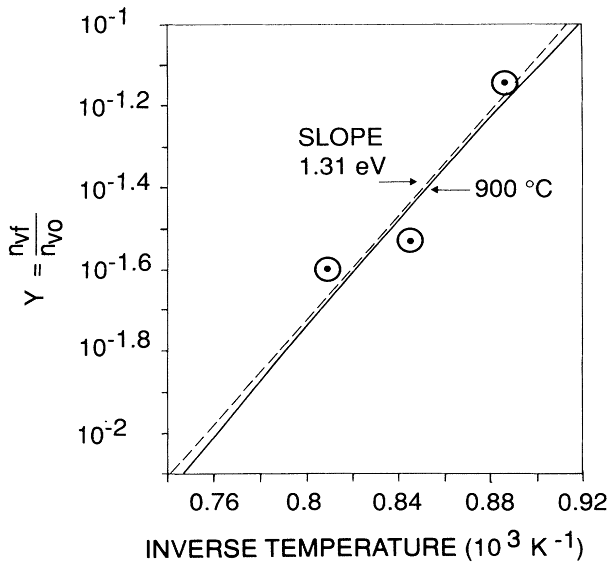

FIG. 6. Annealed vacancy fraction $Y = n_{vf}/n_{v0}$, as a function of inverse annealing temperature for $\Delta E = E_C - E_D = 1.64$ eV. Except for a slight curvature, the relationship is nearly linear and gives a slope of ≈ 1.3 eV at 900 °C.

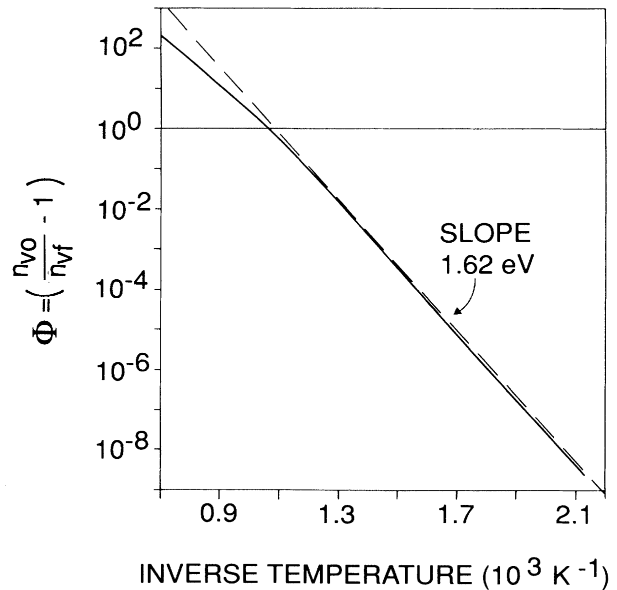

FIG. 7. Parameter ϕ, defined in Eq. (24), as a function of inverse temperature. For the number of activated boron atoms to decrease with increasing annealing temperature, Γ, defined in Eqs. (23) and (28), must increase faster with temperature than ϕ.

$$n_A = R_A n_{d0} , \tag{35}$$

where R_A is the activation ratio from Eq. (27) and n_{d0} the implanted boron-ion dose, which is 1.75×10^{14} cm^{-2} according to Table I. In turn, the number of donors n_D per cm^2 follows as

$$n_D = n_{vf}/h , \tag{36}$$

where it is again assumed that all the uncombined vacancies n_{vf} take part to form vacloids, each consisting out of an average of h vacancies. However, to use $n_A - n_D$ to derive values for the appropriate boron constants is extremely difficult. To do this a model is needed which accurately describes the diffusion and agglomeration of the uncombined vacancies. From a previous analysis it was deduced that the average number of vacancies, h, per vacloid depends on the annealing cycle employed.[9] The lower the initial annealing temperature, the larger h seemed to be. Thus, for each of the curves shown in Fig. 8, a different value of h is expected, and it is not known, as already mentioned, how to estimate these quantities. In fact, much more research is needed on this aspect of vacancy diffusion and agglomeration as well as the electronic behavior of these entities. For instance, in the preliminary analysis[9] it was assumed that a vacloid can only donate one electron. It may not be the case, and as long as such information is unknown, it will be difficult to estimate the true number of donors which form, during a specific annealing cycle, out of the residual radiation damage.

In the present situation, one can, at least, attempt to estimate some of the quantities involved to determine whether the model may be considered as realistic. The minimum resistivity measured for the boron-doped layers shown in Fig. 2 provides a rough guide. As already mentioned, the parabola was fitted to the data using only the layers annealed at the four lowest temperatures. In the case of the layer annealed at 1100 °C, conduction occurred, at least partly, by holes in the valence band, which owing to their higher mobility, should cause a lower resistance to be measured. The other layers relate to variable-range-hopping conduction, and the resistances increase with a decrease in the uncompensated acceptor density. Thus by parabolic extrapolation the annealing temperatures at which the latter quantity is small enough to be neglected may be roughly approximated. The effective "sheet resistance," measured on the same diamonds in their virgin state after applying the same type of contacts, was in the order of 10^{18} Ω/□. From the parabola this resistance is expected for anneals at either 845 or 1130 °C. It was thus assumed that at these temperatures n_A and n_D from Eqs. (35) and (36) can be equated. Knowing the annealing temperatures, one can solve, in each case, for $\kappa n_{v0}/\varphi$ [using Eq. (33)], then for n_{vf}/n_{v0} [Eq. (12)], and for ϕ [Eq. (24)]. From Eqs. (28) and (29), Γ, at temperature T, may be written as

$$\Gamma(T) = \left[\frac{\kappa n_{v0}}{\varphi}\right] A(T) , \tag{37}$$

where

$$A(T) = \left[\frac{\varphi_{0d}}{\kappa_{0d} n_{v0}}\right] \exp\left[\frac{\Delta E_d}{kT}\right] . \tag{38}$$

Accordingly, the donor-acceptor equivalence at the temperatures of 845 and 1130 °C gives the following equations, where $A(T)$ is indicated by A_1 and A_2 and the vacancies per vacloid by h_1 and h_2, respectively:

at 845 °C,

$$h_1 = 300.14 + 851.13 A_1 ; \tag{39}$$

at 1130 °C,

$$h_2 = 19.40 + 104.73 A_2 . \tag{40}$$

If one looks at the equation for $A(T)$ and compares the preexponential factor to the equivalent one for the self-interstitials, derived above [i.e., the inverse of the preexponential factor in Eq. (33)], one would expect it to be less than unity. Furthermore, the conclusion has been reached that ΔE_d is small or even negative. A_1 and A_2 should thus be positive quantities having values between unity and zero. From this reasoning it follows that $300 < h_1 < 1150$ and $20 < h_2 < 125$. According to a previous analysis, using Fermi-Dirac statistics,[9] it was concluded that the average number of vacancies per vacloid, for similarly ion-damaged layers, which were subjected to initial anneals at 500 and 1200 °C, was 2410 and 104, respectively. In comparison, the values for h_1 and h_2 compare favorably, even for A_1 and A_2 larger than unity.

IV. DISCUSSION

Although the present, scarce availability of experimental data makes it impossible to derive values for all the constants involved in this theoretical model, the values estimated, in terms of the present knowledge, seem reasonable and correlate well with each other, as well as with previous calculations. This is quite remarkable in view of the approximations which were made when the model was applied to the existing data. In effect, the further assumption was also made that the diamonds heated instantaneously to the first annealing temperature. Time is required to reach these temperatures, and quite a large amount of interstitial diffusion may have occurred while the implanted surface layer heated up. Nevertheless, a basic framework has been established which provides new insights and suggests numerous new routes for experimental investigation.

Probably the most interesting aspect of the model is the assumption that two activation energies are involved for each interstitial-vacancy combination reaction, namely, the diffusion energy and actual combination energy. Usually, the analysis for point-defect interactions in solids is done solely in terms of diffusion activation.[18] For example, in diamond, Palmer[19] and Clark and Palmer[17] applied the latter logic to derive an activation energy of 1.3 eV for self-interstitial diffusion in diamond. A separate activation energy for combination was not considered. Their analysis was based on the removal of the

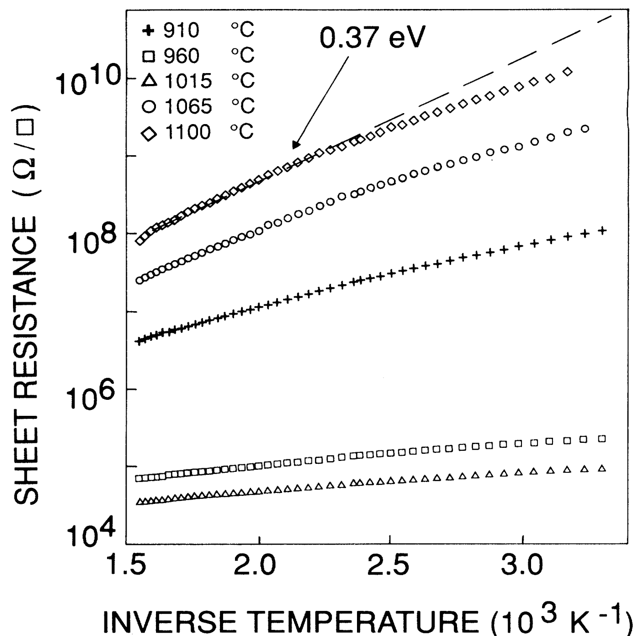

FIG. 8. Sheet resistance as a function of inverse temperature for boron-doped layers generated after annealing at different initial temperatures. The layers were first coimplanted, at liquid nitrogen temperature, to the doses shown in Table I. Except for the layer annealed at 1100 °C, which showed a region of activated electrical conduction at 0.37 eV, the other layers could be described in terms of variable-range-hopping conduction (from Ref. 11).

GR1 optical absorption center, which is currently accepted as a fingerprint of the vacancy in diamond.[2] In other words, the decrease in vacancy concentration with temperature should, according to the present model, have followed the relationship shown in Fig. 8. Although this is, most probably, fortuitous, it is interesting that the effective activation energy, derived from this curve, is, to all purposes, the same as they have found. The probability thus exists that the 1.3 eV, reported by Clark and Palmer, may not refer to the actual activation energy of interstitial diffusion, but rather to the difference in the combination and diffusion energies.

Finally, it should be noted that the model makes physical sense. Two interstitial types are involved. For the interstitial with the highest activation energy, the rate at which the process, controlled by this energy, occurs will increase faster with temperature than for the interstitial with the corresponding lower energy. Thus, if the self-interstitial has a higher vacancy-combination energy than the boron interstitial, it will fill vacancies faster at higher temperatures than the boron can. If, at the same time, the boron interstitials have a larger activation energy for diffusion, the rate at which they can escape at higher temperatures, from the ion-damaged layer, will be greater than for the self-interstitials.

V. CONCLUSION

In an attempt to understand the point-defect interactions which occur when annealing diamond after ion implantation at low target temperatures, a model has been developed based on reaction-rate theory. For each interstitial-vacancy interaction, two activation energies were considered, namely, the diffusion energy and combination energy. A comparison of the equations with existing data gives consistent results and also describes how the self-interstitials and dopant interstitials compete with each other to fill vacancies. In particular, the observed decrease in boron acceptor activation compared to the improvement in self-interstitial–vacancy combination, when increasing the annealing temperature, can be satisfactorily explained.

[1] W. J. King and C. M. Kellet, U.S. Patent No. 3 383 567 (1968).
[2] For a review, see C. D. Clark, E. W. J. Mitchell, and B. J. Parsons, in *The Properties of Diamond,* edited by J. E. Field (Academic, New York, 1979), p. 23.
[3] C. D. Clark, P. J. Kemmey, and E. W. J. Mitchell, Discuss. Faraday Soc. **31**, 96 (1961).
[4] H. B. Dyer and P. Ferdinando, Br. J. Appl. Phys. **17**, 419 (1966).
[5] J. F. Prins, Phys. Rev. B **31**, 2472 (1985).
[6] J. F. Prins, T. E. Derry, and J. P. F. Sellschop, Phys. Rev. B **34**, 8870 (1986).
[7] J. F. Prins, Phys. Rev. B **38**, 5576 (1988).
[8] J. F. Prins, Nucl. Instrum. Methods B **35**, 484 (1988).
[9] J. F. Prins, Phys. Rev. B **39**, 3764 (1989).
[10] R. A. Spits, T. E. Derry, J. F. Prins, and J. P. F. Sellschop, Nucl. Instrum. Methods B **51**, 247 (1990).
[11] J. F. Prins, Nucl. Instrum. Methods (to be published).
[12] J. F. Prins, Mater. Sci. Eng. B (to be published).
[13] J. F. Ziegler, J. P. Biersack, and U. Littmark, *The Stopping and Range of Ions in Solids* (Pergamon, New York, 1985).
[14] N. F. Mott, Philos. Mag. **19**, 835 (1969).
[15] N. F. Mott and E. A. Davies, *Electronic Processes in Non-Crystalline Materials* (Clarendon, Oxford, 1971).
[16] J. Bernholc, A. Antonelli, T. M. Del Sole, Y. Bar-Yam, and S. T. Pantelides, Phys. Rev. Lett. **61**, 2689 (1988).
[17] C. D. Clark and D. W. Palmer, in *Proceedings of the Fourth Symposium on Reactivity of Solids, 1960* (Elsevier, Amsterdam, 1960), p. 436.
[18] W. M. Lomer and A. H. Cottrell, Philos. Mag. **46**, 711 (1955).
[19] D. W. Palmer, Ph.D. thesis, Reading University, 1962.